Applied Catalysis B: Environmental 194 (2016) 22–31

Contents lists available at ScienceDirect

Applied Catalysis B: Environmental

journal homepage: www.elsevier.com/locate/apcatb

Methane combustion over bimetallic Ru-Re/γ-Al_2O_3 catalysts: Effect of Re and pretreatments

Janina Okal*, Mirosław Zawadzki, Katarzyna Baranowska

Institute of Low Temperature and Structure Research, Polish Academy of Sciences, Okólna 2, 52-422 Wrocław, Poland

ARTICLE INFO

Article history:
Received 17 February 2016
Received in revised form 12 April 2016
Accepted 19 April 2016
Available online 23 April 2016

Keywords:
Bimetallic Ru-Re catalyst
Methane combustion
Effect of pretreatment
Effect of rhenium

ABSTRACT

In this paper, we have presented the results of the studies on methane combustion over bimetallic Ru-Re/γ-Al_2O_3 catalysts containing 1 or 3 wt.% of Re, and their comparison with those obtained over 5% Ru/γ-Al_2O_3 catalyst. The catalytic activity was examined on reduced catalysts and then aged in air at 500 °C under O_2-rich conditions. All catalysts were characterized by various methods such as BET, XRD, TEM, HAADF-STEM, EDS and H_2-TPR in order to correlate their activity with their physiochemical properties. A positive effect of the ageing treatment on the catalytic performance was observed for the both bimetallic Ru-Re catalysts but not for the Ru catalyst. The methane oxidation rate over the aged Ru-Re catalysts was about 5–10 times higher compared to that of the aged Ru catalyst. Characterization data show that at ageing temperature of 500 °C small Ru or RuRe particles were transformed into larger RuO_2 particles and/or highly dispersed ReO_x species strongly interacting with γ-alumina. The mean crystallite size of RuO_2 decreased from 25 to 14 nm when the Re loading had been changed from 1 to 3 wt.%, while in the monometallic Ru catalyst it was higher and amounted to 30 nm. Among the reduced catalysts, the 5%Ru-1%Re catalyst exhibited the highest activity for combustion of methane. Also, for this sample apparent activation energy (104 kJ mol^{-1}) was lower as compared to that of the monometallic Ru catalyst (116 kJ mol^{-1}), indicating that Re slightly lowers the methane activation barrier. For the Ru as well as bimetallic Ru-Re catalysts an instability of methane conversion as a function of time (80 h) at a given temperature (500 °C) was observed. The instability was associated with slow formation of larger RuO_2 crystallites (40–45 nm) during the course of the reaction. In summary, the addition of Re improves the catalytic activity of the Ru/γ-Al_2O_3 catalysts for methane combustion but thermal stability of the bimetallic samples is similar to that of the unpromted Ru catalyst.

1. Introduction

Methane is a secondary product of various industrial processes and a potent greenhouse gas (~25 times stronger than CO_2). It is also used as an energy source in different applications including gas turbines and natural gas fuelled vehicles. During these combustion processes, some unburned methane and other compounds (NO_x, hydrocarbons, CO) may be released to the environment, and various types of catalytic converter have been developed to remove them. Among the hydrocarbons, methane is the most resistant to oxidation, as reflected by the relatively high temperatures required to carry on the combustion process. The low reactivity of methane is related to the symmetry of its molecule and difficulty with its adsorption on different catalytic surfaces in comparison with those of higher alkanes [1].

Noble metal catalysts (Pd, Pt, Au, Rh) are a common choice of an active component in complete oxidation of methane [2,3]. Among them, supported Pd catalysts, especially Pd supported γ-Al_2O_3 catalysts that demonstrate the highest activity, are the most attractive catalytic materials for methane combustion [4–8]. However, using palladium has some drawbacks, including large hysteresis effects due to palladium oxide transformation into metallic palladium and deactivation at higher temperature due to sintering. Moreover, palladium based catalysts are extremely sensitive to sulfur poisoning and their activities toward CH_4 destruction deteriorate very quickly in the presence of SO_2 or SO_3. In order to stabilize a catalyst, an addition of another noble metal such as Pt, Rh, Ru, etc. has been proposed by several authors. Bimetallic systems, especially those based on Pd-Pt, have been frequently studied in methane combustion since they usually show better performance than that of monometallics in this reaction [9,10]. Moreover, the stability of

* Corresponding author.
E-mail address: J.Okal@int.pan.wroc.pl (J. Okal).

http://dx.doi.org/10.1016/j.apcatb.2016.04.038
0926-3373/

methane conversion makes this type of catalysts more attractive than monometallic Pd catalyst [11]. In addition to Pd-Pt-based catalysts, other noble-metal bimetallic catalysts have also been investigated in methane combustion, for instance Pd-Rh/Al_2O_3 [12] or Pd-Au catalysts [13].

Compared with Pd or Pt-based catalysts, Ru-based catalysts for CH_4 oxidation attracted less interest mainly due to their limited high-temperature stability [14]. Catalytic oxidation of various types of volatile organic compounds (VOCs) over Ru catalysts was also not frequently studied [15]. Ryu et al. [16] reported the effects of Ru or Rh addition to Pd/Al_2O_3 catalysts used in methane combustion. They found a beneficial effect of Ru addition, both in the activity and especially in the resistance to sulfur-induced deactivation. This effect was attributed to an improved dispersion of Pd and to the intrinsic resistance of Ru to sulfur poisoning. However, they did not find any beneficial effect of Rh addition. Effects of Ru or Rh addition on the activity and sulfur tolerance of Pt/ZrO_2 catalyst for oxidation of methane were also investigated recently [17]. It was found that Ru-Pt/ZrO_2 catalysts exhibited high activity for methane oxidation at low temperature below 400 °C and the catalysts did not deactivate in the presence of SO_2. Hence, bimetallic catalysts containing Pd or Pt and Ru metal are suitable for oxidation of methane in containing sulfur compounds streams. The role of Ru was to maintain Pt in a high oxidation state in which Pt exhibits high activity for methane oxidation. Under the same conditions, Ru/ZrO_2 did not show any significant activity for methane oxidation [17]. Our recent studies performed over Ru supported on the $ZnAl_2O_4$ spinel [18] showed however, that the specific activity of ruthenium in methane combustion was comparable with that of reported for Pt catalysts, but it was lower than that reported for the most active Pd catalysts [19]. Comparative studies of methane combustion over Pt, Pd and Rh/Al_2O_3 catalysts showed that in an oxidizing feed stream, the catalytic activity ranking is given by Pd > Rh > Pt [20].

In this study, we investigated low temperature methane combustion over bimetallic Ru-Re/γ-Al_2O_3 catalysts and we compared the catalytic results with those obtained over Ru/γ-Al_2O_3 catalyst and two commercial Ru/Al_2O_3 (Fluka) and Pd/Al_2O_3 (Degussa) catalysts. The large differences in the electronegativities of ruthenium and rhenium suggest that strong modification of redox properties of the noble metal could be obtained in the Ru-Re/γ-Al_2O_3 samples. Moreover, reduction of rhenium is enhanced by the presence of ruthenium as **it** was reported by Ma and He [21,22] and Baranowska et al. [23]. In addition, a beneficial effect of rhenium addition to ruthenium catalyst for oxidation reactions has been reported recently [24]. It was found that addition of 1 or 3 wt.% of rhenium to 5 wt.% Ru/γ-Al_2O_3 catalyst decreased the light-off temperature for propane combustion and improved the specific reaction rates, while at higher concentration (9.2 wt.% Re) led to lower conversions. The improvement of the activity was related to better reducibility of the metal oxide species and higher dispersion of an active RuO_x phase [24]. Moreover, Re-modified catalysts were much more stable during propane oxidation in O_2-rich reaction conditions [24,25]. It can be noted however, that oxidation of short-chain hydrocarbons with 2–4 carbons on noble metal catalysts is usually completed at temperature below 400 °C, but complete catalytic oxidation of methane is not possible at this temperature [14]. Therefore, using rhenium as a catalyst promoter for oxidation reactions may be questioned because of the possibility of formation of volatile rhenium oxides at high temperature [26]. This may be the case when a high loading of rhenium supported on alumina is used [27]. In our case, the low rhenium loading (up to 3 wt.%) in bimetallic Ru-Re catalysts leads to a strong interaction between ReO_x species and the alumina support, precluding formation of volatile rhenium compounds.

Motivated by our recent studies, in this paper the performance of two Ru-Re/γ-Al_2O_3 catalysts containing 5 wt.% Ru and 1 or 3 wt.% Re in combustion of methane has been reported, together with structure characterization of fresh and used catalysts, using BET, XRD, TEM, HAADF-STEM, EDS and H_2-TPR. Before catalytic testing, the Ru-Re catalysts were pretreated with two different methods: one was hydrogen treated (reduced catalyst) and the other was air treated (aged catalyst). The effect of the rhenium addition and the pretreatment procedure on the methane combustion over Ru-Re/γ-Al_2O_3 catalysts activity was studied by obtaining light-off curves. It should be noted that bimetallic Ru-Re catalysts have been reported only for hydrogenolysis of glycerol [21,22], hydrogenation of amides [28] and succinic acid [29], but to our best knowledge, no examples are available for combustion of methane. Previously, we investigated the performance of the reduced Ru-Re/γ-Al_2O_3 catalysts in combustion of propane [24,25], the total oxidation of which is however easier than that of methane.

2. Experimental

2.1. Catalyst preparation

Bimetallic Ru-Re and monometallic (Ru, Re) catalysts were prepared by incipient wetness impregnation with $Ru(NO)(NO_3)_3$ and NH_4ReO_4 (all Alfa Aesar) precursors as described previously [23]. γ-Al_2O_3 used as a support material had specific surface area of 178 m^2/g, total pore volume of 0.51 cm^3/g and mean pore diameter of 7.8 nm and it was provided by Puralox. After impregnation, the samples were dried in air at 110 °C for 20 h and reduced in H_2 flow at 500 °C for 4 h. Then part of the reduced samples were aged by thermal treatment in static air at 500 °C for 3 h (with heating rate of 5 °C/min) in order to completely oxidise the metal phase. The catalysts treated with hydrogen were denoted as Ru-Re(red) and those with air as Ru-Re(aged).

Commercial catalysts, 5% Ru/Al_2O_3 and 5% Pd/Al_2O_3, were purchased from Fluka and Degussa, respectively. Prior to catalytic tests or characterization the commercial catalysts were treated similarly as those prepared in the laboratory.

2.2. Catalyst characterization

Nitrogen adsorption-desorption measurements, performed at liquid nitrogen temperature by using an Micromeritics ASAP 2020 instrument, were applied to determine specific surface area S_{BET} (multi-point BET method), total pore volume V_p (at $P/P_o \geq 0.95$) and pore size distribution of the prepared samples. The pore size distribution and mean pore diameter (D_p) were calculated from N_2-desorption isotherm by Barrett–Joyner–Halenda (BJH) method. Prior to the analysis, the samples were degassed at 350 °C for 4 h.

Temperature programmed reduction (TPR) measurements were carried out with a Micromeritics Autochem 2910 apparatus equipped with a thermal conductivity (TCD) detector. Experiments were performed by heating a sample (50 mg) from room temperature to 800 °C with the heating rate of 5 °C/min in 5 vol% H_2 in Ar at a flow rate of 30 ml/min. Before all TPR measurements the surface of the catalysts was first cleaned by heating them in Ar flow for 3 h at 200 °C.

The crystal structure of the catalyst samples was determined by XRD (X'Pert PRO PANalytical powder diffractometer, CuKα radiation). Morphology and microstructure was investigated by TEM (Philips CM-20 SuperTwin operating at 200 kV and providing 0.25 nm resolution). TEM images and SAED patterns were analyzed with the Digital Micrograph programme. High-angle annular dark field scanning transmission electron microscopy (HAADF-STEM) measurements of the aged samples were performed with a FEI Titan3 G2 60-300 microscope at 300 kV using a HAADF detector and energy dispersive X-ray spectroscopy with FEI ChemiSTEM tech-

nology (at Technische Universiteat Graz, Austria). The elemental ratios of Ru/Re for the fresh and used samples were also confirmed by energy dispersive spectroscopy EDS (EDAX Pegasus XM4 spectrometer installed on FEI NovaNanoSEM 230 microscope).

2.3. Catalytic oxidation of methane

Combustion of methane was measured in a continuous flow fixed bed reactor at atmospheric pressure and variable temperature. 100 mg of the sample, pretreated in hydrogen or thermally aged in air, was loaded in the quartz tube reactor (i.d. = 8 mm, long = 350 mm) between two layers of quartz beds to assure uniform gas flow in the catalyst bed. The quartz tube was placed in a furnace equipped with a temperature controller. A gas mixture of 0.8 vol% CH_4 in dry synthetic air, which is a mixture of nitrogen (78 vol%) and oxygen (22 vol%), was fed to the reactor at a space velocity of 60,000 h^{-1} for all types of activity tests. Before measuring the conversion as a function of temperature, the catalyst was activated in the gas mixture from RT to 300 °C (the heating rate of 2 °C/min) and stabilized at this temperature for 1 h. Then, the temperature was lowered to 150 °C and measurements were performed as the samples were heated stepwise usually in the temperature range 150–600 °C. The analyses were made at each temperature until steady-state activity was obtained, and at least two analyses were taken and data averaged. The products were analyzed on line using a gas chromatograph (PerkinElmerARNEL Clarus 500) equipped with thermal conductivity and flame ionization detectors.

3. Results and discussion

CH_4 oxidation activity measurements were conducted to establish the differences in the rate resulting from different pretreatments (reduction, ageing) of the bimetallic Ru-Re and monometallic Ru catalysts supported on γ-alumina. The catalytic performances of these samples were compared with those of commercial catalysts, 5% Ru/Al_2O_3 and 5% Pd/Al_2O_3. Numerous literature data show that alumina is the most suitable support for methane oxidation [5,7,30,31], due to its chemical and physical stability and high mechanical resistance, the surface area of which is quite high (up to about 1000 °C). Combustion of methane in oxygen-rich atmosphere was tested over two Ru-Re/γ-Al_2O_3 catalysts containing 5 wt.% Ru and 1 or 3 wt.% Re, corresponding to the Ru:Re atomic ratio of 90:10 and 75:25, respectively. The ageing temperature of 500 °C was selected since we recently found that ruthenium supported on $ZnAl_2O_4$ spinel aged in air at this or higher temperature showed a very good thermal stability during methane combustion reaction [32]. Structural characterization of the initial state of the Ru-Re or Ru in the air-aged samples was determined by BET, TEM, XRD, H_2-TPR and STEM-EDS.

3.1. Structure characterization of the reduced Ru-Re/γ-Al_2O_3 catalysts

The main morphological characteristics of the Ru-Re/γ-Al_2O_3 catalysts before oxidation treatment were given in our previous study [23]. H_2 chemisorption studies indicated that the hydrogen uptake (H/Ru) values obtained on the Ru_{90}-Re_{10}/γ-Al_2O_3 and Ru_{75}-Re_{25}/γ-Al_2O_3 catalysts (0.57 or 0.74, respectively) were higher than that of the monometallic Ru catalyst (0.52). The average metal particle size evaluated by a direct observation by HRTEM was 1.3 nm for the Ru_{90}-Re_{10} catalyst and 1.1 nm for the Ru_{75}-Re_{25} catalyst and it was slightly smaller than that of the monometallic Ru catalyst (1.4 nm) [23].

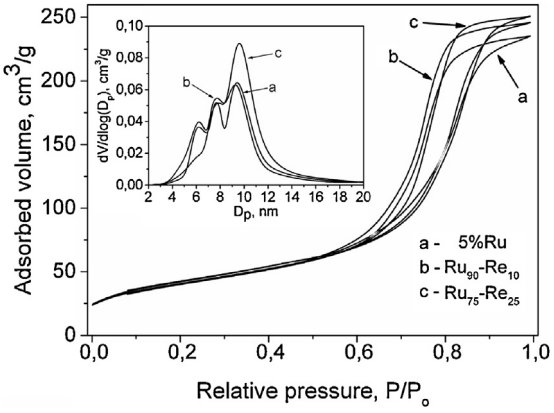

Fig. 1. N_2 adsorption-desorption isotherms of the air-aged 5% Ru/γ-Al_2O_3 catalyst (a) and Ru-Re/γ-Al_2O_3 catalysts with Ru/Re atomic ratio of 90:10 (b) and 75:25 (c) with corresponding pore size distributions (*as inset*).

3.2. Composition, texture and structure of the aged Ru-Re/γ-Al_2O_3 catalysts

The atomic ratios obtained by using EDS analysis for the aged Ru-Re/γ-Al_2O_3 catalysts were compared with those obtained for the reduced samples (Table 1). For the both reduced catalysts the Ru:Re atomic ratios were slightly lower when compared with the nominal ones and only small deviations at various points at the samples were observed. On the basis of the used multi-point EDS analysis we could not, however, prove that Ru and Re are in one bimetallic nanoparticle. EDS results of the aged catalysts indicate that the Ru:Re atomic ratios were close to that of in the fresh reduced samples, indicating that no noticeable loss of Ru and Re (as volatile RuO_4 or Re_2O_7 oxide, respectively) occurred during this high temperature oxidation treatment.

Texture properties of the catalysts after air-ageing treatment at 500 °C were examined by nitrogen adsorption-desorption measurements as presented in Fig. 1. All the isotherms represent the type IV with a well-defined hysteresis loop of type H1, which is typically observed for materials with mesoporous structure. The steep increases of the adsorption volume at P/P_o (0.6–0.9) are due to capillary condensation of nitrogen in the mesopores. The inset of Fig. 1 shows a typical BJH pore size distribution for the studied catalysts. Detailed textural properties of the monometallic Ru and bimetallic Ru-Re catalysts as well as commercial Ru/Al_2O_3 and Pd/Al_2O_3 catalysts are listed in Table 2. BET surface area of the air-aged monometallic Ru catalyst amount to 145 m^2/g i.e., about 20% less than the surface area of the reduced sample or the bare alumina support (178 m^2/g). Similar loss of the BET surface areas was observed for the both air-aged bimetallic Ru-Re catalysts. The loss of the BET surface area of the studied samples is mainly related to the changes in the pore structure of the catalysts. As can be seen the total pore volumes drop from about 0.45 cm^3/g to about 0.38 cm^3/g after oxidation treatment of the catalysts at 500 °C. Probably the oxidized metal species (RuO_2, Re_2O_7) are located inside the pores or some alumina pores are blocked by larger RuO_2 particles that grew on the support surface. Most likely this blockage is more severe for the smallest pores of the given catalyst. This effect on the smallest pores can eventually be seen as an increase of mean pore sizes. It can be noted that for the commercial Ru/Al_2O_3 catalyst, with the same Ru loading as the laboratory prepared monometallic Ru catalyst, the decline of S_{BET} after ageing treatment was higher and amounted to about 31% (Table 2). Our recently reported volumetric O_2 adsorption data [24] revealed that temperature of 150 °C was sufficient to complete oxidation of the metal phase in the bimetallic Ru-Re/γ-Al_2O_3 catalysts as well as in the monometallic Ru/γ-Al_2O_3 catalyst.

Table 1
Nominal Ru:Re atomic ratios and those obtained by EDS analysis of the reduced at 500 °C, air-aged at 500 °C and used in the methane combustion Ru-Re/γ-Al_2O_3 catalysts.

Catalyst	Actual metal loading (wt%)[a]		Ru:Re atomic ratio (nominal)	Ru:Re atomic ratio (EDS)			
	Ru	Re		Fresh catalysts		After catalytic tests up to 600 °C	
				Reduced	Air-aged	Reduced	Air-aged
Ru_{90}-Re_{10}/γ-Al_2O_3	4.6 ± 0.9	0.8 ± 0.2	90:10 = 9	8.43	8.65	8.69	8.21
Ru_{75}-Re_{25}/γ-Al_2O_3	5.4 ± 1.1	2.3 ± 0.5	75:25 = 3	2.57	2.45	2.60	2.53

[a] Measured by the ICP-AES method [23].

Table 2
Texture properties of the fresh reduced and air-aged catalysts supported on the γ-Al_2O_3.

Catalyst		Reduced samples at 500 °C			Air-aged samples at 500 °C			Re[c] (nm^2)
		S_{BET} (m^2/g)	D_p[a] (nm)	V_p[b] (cm3/g)	S_{BET} (m^2/g)	D_p[a] (nm)	V_p[b] (cm3/g)	
5%Ru	fresh	183	7.8	0.45	145	7.8	0.37	–
	used[d]	*(172)*	*(7.8)*	*(0.45)*	*(148)*	*(7.9)*	*(0.40)*	
Ru_{90}-Re_{10}	fresh	174	7.8	0.45	149	7.7	0.38	0.23
	used[d]	*(165)*	*(7.8)*	*(0.41)*	*(148)*	*(7.7)*	*(0.40)*	
Ru_{75}-Re_{25}	fresh	185	7.8	0.44	147	8.2	0.39	0.72
	used[d]	*(159)*	*(7.8)*	*(0.41)*	*(144)*	*(8.3)*	*(0.39)*	
5%Ru (Fluka)	fresh	129	5.0	0.21	90	5.6	0.17	–
	used[d]	–	–	–	*(89)*	*(5.7)*	*(0.17)*	
5%Pd (Degussa)	fresh	316	3.8	0.30	–	–	–	–
	used[d]							

[a] Mean pore diameter.
[b] Total pore volume.
[c] ReO_x surface density (ReO_x nm^{-2}) in the aged catalysts.
[d] Texture properties of the used catalysts measured after stability tests.

Table 3
Influence of the treatment on the phase composition of the monometallic Ru/γ-Al_2O_3 and bimetallic Ru-Re/γ-Al_2O_3 catalysts. XRD and TEM data for fresh catalysts and XRD data for the samples after methane combustion.

Catalyst	Thermal treatment	Fresh catalysts			Used catalyst
		Ru^0 particle size from XRD (nm)	RuO_2 particle size from XRD (nm)	TEM observation; phase/particle size	RuO_2 particle size from XRD (nm)
5% Ru	H_2/500 °C/4h	n.d.[a]	–	Ru^0, 1–4.5 nm	25
	Air/500 °C/3h	–	30	RuO_2,large irregular agglomerates up to 100 nm	32
Ru_{90}-Re_{10}	H_2, 500 °C/4h	n.d.	–	RuRe particles 1–2.5 nm	26
	Air, 500 °C/3h	–	25	RuO_2, large irregular agglomerates up to 50 nm	31
Ru_{75}-Re_{25}	H_2, 500 °C/4h	n.d.	–	RuRe particles, 1–2 nm	27
	Air, 500 °C/3h	–	14	RuO_2, separated small crystalites	23
5%Ru (Fluka)	H_2, 500 °C/4h	14	–	n.m.[b]	35
	Air, 500 °C/3h	–	21	n.m.	38

[a] Not detected.
[b] Not measured.

TEM and XRD studies showed that the oxidized metal (Ru or RuRe) species were amorphous and highly dispersed but at higher temperature 250 °C these species transformed into crystalline RuO_2 oxide and highly dispersed ReO_x species [24]. The Re surface densities calculated from the measured BET surface area and the rhenium loading in the aged bimetallic Ru-Re catalysts are listed in the last column of Table 2. The density corresponding to the monolayer capacity (monolayer surface capacity is defined as the maximum amount of two-dimensional metal in contact with the oxide support) on γ-Al_2O_3 support has been reported to be 2.3 Re atoms/nm^2 [33]. Thus, for the aged bimetallic Ru_{90}-Re_{10} and Ru_{75}-Re_{25} catalysts the Re surface density is rather low and amount to about 10% or 31% of the monolayer coverage, respectively (Table 2).

3.2.1. X-ray diffraction studies

XRD patterns of the monometallic Ru and bimetallic Ru-Re catalysts aged at 500 °C are presented in Fig. 2. The all patterns show the characteristics reflections corresponding to RuO_2 oxide (JCPDS 88-0322), with (110), (101) and (211) as the prevailing primary orientations. The mean crystallite size of Ru oxide, calculated from the line broadening of the most intense (110) reflection of RuO_2 oxide

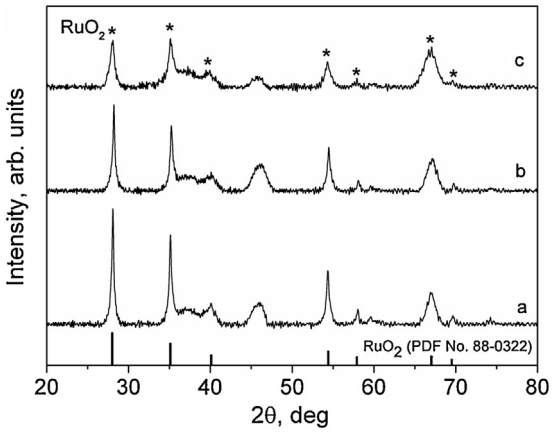

Fig. 2. X-ray diffraction patterns of the monometallic 5% Ru/γ-Al_2O_3 (a) and bimetallic Ru_{90}-Re_{10}/γ-Al_2O_3 (b) and Ru_{75}-Re_{25}/γ-Al_2O_3 (c) catalysts aged at 500 °C for 3 h. Standard diffraction pattern of RuO_2 (File no. 88-0322) is also presented.

at $2\theta = 28.09^{\circ}$ amounted to 30 nm for the monometallic Ru catalyst and 25 nm or 14 nm for the Ru_{90}-Re_{10} and Ru_{75}-Re_{25} catalysts, respectively (Table 3). Evidently, the addition of Re to the Ru/γ-Al_2O_3 catalyst causes smaller aggregation of the Ru phase in the used oxidizing conditions. No evidence of any Re oxide phase was found for the aged bimetallic catalysts, although the EDS results confirm that all Re is present in these samples (Table 1). Nevertheless, rhenium oxide in the aged bimetallic Ru-Re catalysts may exist as highly dispersed phase not giving detectable diffraction peaks. Our recently published XPS data, obtained for the bimetallic Ru_{75}-Re_{25}/γ-Al_2O_3 catalyst oxidized at 250 °C [24], show that Re is oxidized to Re^{4+} (30%), Re^{6+} (20%) and Re^{7+} species (50%). On the other hand, XPS data, obtained for the monometallic 1% and 10.4% Re/γ-Al_2O_3 catalysts, show that at 500 °C all Re was oxidized to Re^{7+} species [34]. Additionally, for the bimetallic Ru_{75}-Re_{25} catalyst oxidized at 250 °C [24] as well as monometallic Re/γ-Al_2O_3 catalysts oxidized at 500 °C [34], the XPS determined Re/Al atomic ratios increased after these oxidation treatments indicating a large spreading of the rhenium oxide species on the support surface. Spreading of the rhenium phase in the monometallic Re/γ-Al_2O_3 samples was also confirmed by the extensive HRTEM studies [27,34].

3.2.2. TEM and STEM-HAADF studies

Fig. 3 shows representative TEM images and a SAED pattern (included as an inset) of the monometallic Ru and bimetallic Ru-Re catalysts aged in air at 500 °C. In the TEM image of the Ru/γ-Al_2O_3 catalyst (Fig. 3a) a large irregular conglomerate with the size of about 90 nm × 70 nm is seen, which can be identified as crystalline RuO_2 oxide based on the SAED (inset to Fig. 3a) analysis. In the aged bimetallic Ru_{90}-Re_{10} catalyst (Fig. 3b) the ruthenium phase also forms agglomerates but of a smaller size, not exceeding 50 nm. The XRD data also show that crystallite size of RuO_2 is smaller in the bimetallic Ru_{90}-Re_{10} catalyst (25 nm) in comparison with that of the Ru catalyst (30 nm). In the aged bimetallic Ru_{75}-Re_{25} catalyst (Fig. 3c) the Ru phase is not so agglomerated but it forms separate smaller RuO_2 crystallites. These RuO_2 crystallites exhibit characteristic rod-like shapes with particle dimensions not exceeding 40 nm × 8 nm. The high-resolution transmission electron microscopy (HRTEM) image in the inset shows a very thin crystallite (20 nm × 6 nm) with lattice fringes of distances 0.32 nm that well correspond to the (110) lattice plane of RuO_2 oxide. It should be noted that the localization of the oxidized rhenium phase in the aged bimetallic Ru-Re catalysts can not be carried out by conventional TEM/HRTEM imaging because it is probably highly dispersed. Since high-angle annular dark field (HAADF) imaging in the scanning transmission electron microscope (STEM) is capable of providing simultaneous structural and chemical information with atomic resolution, we performed characterization of the aged bimetallic Ru_{75}-Re_{25} catalyst using this technique. The HAADF technique was chosen because of the correlation between atomic number and the intensity of the image, therefore it provides a possibility to distinguish heavy elements such as Ru or Re. Fig. 4 shows a high magnification STEM-HAADF image of the aged bimetallic Ru_{75}-Re_{25} catalyst and a corresponding line in the EDS spectrum collected along a RuO_2 particle (a white particle with lattice fringes of distances 0.32 nm), as matched by an arrow. It is clearly visible that the EDS signal from the particle of Ru atoms is intense but some small amounts of Re atoms are also observed. Thus, we can conclude that some separation between ruthenium and rhenium phase occurs during oxidation process. Big, highly crystalline particles are mostly composed of Ru atoms. According to the EDS spectrum of RuO_2, the oxidized Re species may be located on the surface of ruthenium oxide. Additionally, we suppose that the very small white particles (~0.6 nm) situated uniformly on the support around the big RuO_2 crystallite are rhenium oxide species. Simi-

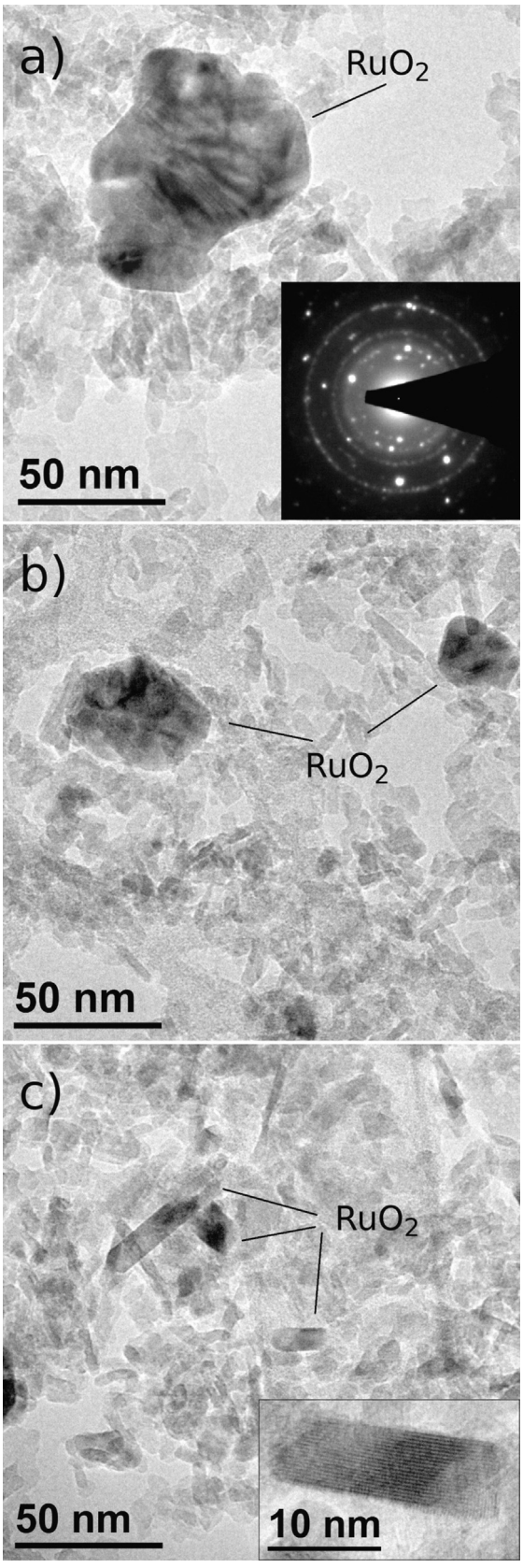

Fig. 3. Representative TEM images and **a** SAED pattern (included as *an inset)* of the monometallic 5% Ru/γ-Al_2O_3 (a) and bimetallic Ru_{90}-Re_{10}/γ-Al_2O_3 (b) and Ru_{75}-Re_{25}/γ-Al_2O_3 (c) catalysts aged at 500 °C for 3 h.

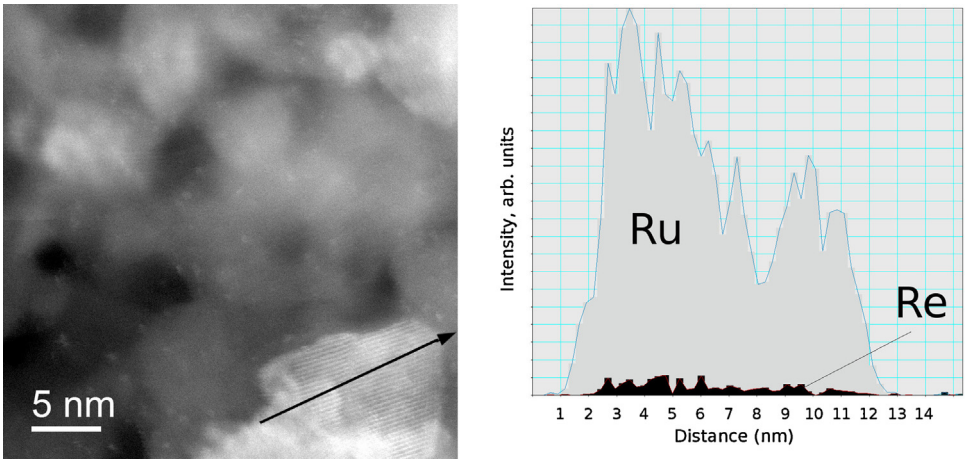

Fig. 4. A high magnification STEM-HAADF image (left) of the aged bimetallic Ru_{75}-Re_{25}/Al_2O_3 catalyst and the EDS spectrum (right) collected from the RuO_2 particle along the line matched by an arrow. The intensive peak in a light grey color corresponds to the amount of the Ru phase and a black one to the rhenium phase.

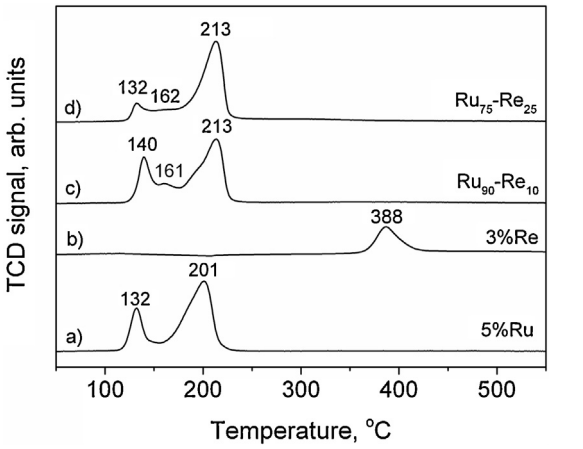

Fig. 5. TPR profiles of the aged at 500 °C the monometallic 5% Ru/γ-Al_2O_3 (a) and 3% Re/γ-Al_2O_3 catalysts (b), and the bimetallic Ru_{90}-Re_{10} (b) and Ru_{75}-Re_{25} catalysts (c).

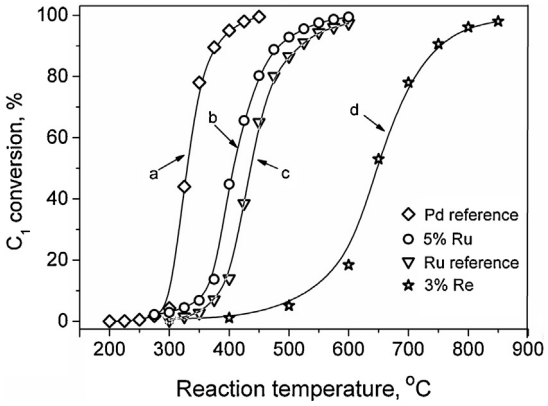

Fig. 6. Methane conversion as a function of temperature over the reduced monometallic samples; the commercial 5% Pd/Al_2O_3 (Degussa) catalyst (a), the laboratory made 5% Ru/γ-Al_2O_3 catalyst (b) the commercial 5% Ru/γ-Al_2O_3 (Fluka) catalyst (c), and the 3% Re/γ-Al_2O_3 catalyst (d). *Experimental conditions*: methane concentration: 0.8% vol. in air, total flow rate: 100 cm^3 min^{-1}; mass of the catalyst: 100 mg, pressure: atmospheric.

lar particle size of the oxidized rhenium species was observed by HRTEM in the 10.4% Re/γ-Al_2O_3 catalyst oxidized at 250–800 °C [27].

Concluding, XRD and TEM characterization data presented in this study evidently show that ageing treatment in air at 500 °C induces a significant thermal sintering of the Ru phase partly inhibited when Re is added to the Ru/γ-Al_2O_3 catalyst (Table 3).

3.2.3. *Temperature-programmed reduction (H_2-TPR)*

In order to investigate reduction behaviour of the studied catalysts, after their treatment in air at 500 °C, H_2-TPR studies were performed as shown in Fig. 5. The TPR profile of the 5% Ru/γ-Al_2O_3 catalyst (profile a) contains two well-resolved reduction peaks, indicating the existence of two kinds of oxidized ruthenium species on the alumina support. The first one, centered at 132 °C, is assigned to the reduction of RuO_2 in a well-dispersed form. The second peak, at about 201 °C, corresponds to reduction of RuO_2 in a crystalline form. This profile is similar to those found in the literature [24,35]. The reduction of oxidized Re species in the 3% Re/γ-Al_2O_3 catalyst occurs at much higher temperature of 388 °C (profile b). The TPR profiles of the bimetallic Ru-Re catalysts show some differences in comparison to the Ru catalyst and contain an additional weak peak at intermediate temperature (161 or 162 °C). Moreover, the most intense reduction peak is shifted to a slightly higher temperature (213 °C) compared with that of the monometallic Ru catalyst (201 °C). The low-temperature peaks observed below 162 °C are attributed to reduction of the Ru species in a well-dispersed state, and the large peak at higher temperature should correspond to co-reduction of the Ru and Re oxide species. We suppose that the promotion of rhenium reduction in the bimetallic catalysts may be interpreted by hydrogen spillover from proceedingly reduced Ru to Re species. This mechanism was previously suggested for other bimetallic catalysts containing Re such as Rh-Re/SiO_2 [36], Ir-Re/SiO_2 [37], and Ru-Re/γ-Al_2O_3 [24]. Note that the apparent intensity of the low-temperature reduction peaks (below 162 °C) in the bimetallic Ru-Re/γ-Al_2O_3 catalysts decreased with the increase in the Re loading from 1% to 3%.

3.3. *Activity measurements: the effect of pretreatment*

The all prepared samples were investigated for their catalytic activity towards methane combustion, and conversion curves as a function of reaction temperature are illustrated in Fig. 6 and 7, while the temperatures required to achieve different degrees of conversion are summarized in Table 4. Under O_2-rich conditions the all Ru containing catalysts showed complete oxidation of CH_4 to CO_2, i.e., no CO was detected. First, methane combustion was carried out over reduced monometallic 5%Ru/γ-Al_2O_3 and 3%Re/γ-Al_2O_3 catalysts in comparison with commercial available

Table 4
Comparison of the catalytic properties of ruthenium during methane combustion over reduced and aged monometallic Ru/γ-Al_2O_3 and bimetallic RuRe/γ-Al_2O_3 catalysts with the Re and commercial Ru and Pd catalysts.

Catalyst	Thermal treatment	Catalytic activity in terms of conversion temperature (°C)			Specific reaction rate (μmol g^{-1} $min-1$)[a]	Apparent activation energy, E_{app} (kJ mol^{-1})
		T_{10}	T_{50}	T_{95}		
3% Re/γ-Al_2O_3	H_2/500 °C/4h	535	650	800	–	–
5% Pd/Al_2O_3 (Degussa)	H_2/500 °C/4h	300	331	403	–	–
5% Ru/Al_2O_3 (Fluka)	H_2/500 °C/4 h	385	438	560	–	120
	Air/500 °C/3h	386	436	555	–	
5% Ru/γ-Al_2O_3	H_2/500 °C/4 h	361	407	525	2.53	116
	Air/500 °C/3h	402	437	550	0.37	121
Ru_{90}-Re_{10}/γ-Al_2O_3	H_2/500 °C/4 h	337	391	506	5.17	104
	Air/500 °C/3h	350	399	525	3.65	105
Ru_{75}-Re_{25}/γ-Al_2O_3	H_2/500 °C/4 h	375	425	600	1.56	114
	Air/500 °C/3h	359	411	538	2.00	117

[a] Specific reaction rate calculated at 350 °C.

catalysts: 5%Ru/Al_2O_3 (Fluka) and 5%Pd/Al_2O_3 (Degussa). As it can be seen from Fig. 6, the both monometallic ruthenium catalysts possessed sufficiently high catalytic performance and the light-off temperature of our 5% Ru/γ-Al_2O_3 catalyst (T_{50} = 407 °C, Fig. 6b) was lower than that of the commercial Ru reference (T_{50} = 438 °C, Fig. 6c). The differences in the catalytic performance could probably be attributed to the differences in the number of exposed active sites in these Ru samples. The mean Ru particle size of the laboratory synthesized Ru catalyst amounts to 1.4 nm, while that determined by XRD for the commercial Ru reference was significantly higher and amounts to 14 nm (Table 3). As expected, at the same reaction conditions the light-off temperatures for the both Ru catalysts were higher as compared to that of the palladium reference catalyst (T_{50} = 331 °C, Fig. 6a). Moreover, complete methane combustion over the 5% Pd/Al_2O_3 catalyst was also observed at much lower temperature of 450 °C, while for the both monometallic 5% Ru catalysts somewhat above 520 °C. These results are in line with the literature data since the Pd-based catalysts are well known to be the most active catalysts for total oxidation of methane [4–8,30,31]. In the presence of excess oxygen, a high level of activity of the Pd catalysts is expected in the 300–500 °C temperature range, due to the presence of palladium in an oxidized state. Most recent literature data show that at low temperature methane oxidation over Pd/Al_2O_3 catalyst the mixed Pd/PdO sites have the highest activity for methane oxidation [4]. On the other hand, monometallic rhenium catalyst was the least active demonstrating its light-off curve, expressed as methane conversion versus temperature, clearly shifted to higher temperature (T_{50} = 645 °C, Fig. 6d).

Fig. 7a illustrates the combustion behaviour of the reduced bimetallic Ru-Re/γ-Al_2O_3 catalysts in comparison with the reduced monometallic Ru/γ-Al_2O_3 catalyst. The monometallic Ru catalyst shows 100% conversion and values of the temperature for conversion of 10%, 50% and 95% (T_{10}, T_{50} and T_{95}) are 361, 407 and 525 °C, respectively (Table 4). Over the bimetallic Ru-Re catalysts methane conversion depends on the composition (Fig. 7a) and the conversion curves shift toward higher temperature when the Re loading increases from 1 wt.% to 3 wt.%. For the most active Ru_{90}-Re_{10} catalyst, the light-off temperature was about 34 °C lower (T_{50} = 391 °C) than that of for the Ru_{75}-Re_{25} catalyst (T_{50} = 425 °C, Table 4). Moreover, only the reduced bimetallic Ru_{90}-Re_{10} catalyst exhibits much better catalytic performance than the reduced 5% Ru/γ-Al_2O_3 catalyst (Fig. 7a). For low-temperature combustion of propane it was found that both bimetallic Ru_{90}-Re_{10} and Ru_{75}-Re_{25} catalysts exhibited better catalytic performance (T_{50} = 160 °C or 173 °C, respectively) than the monometallic 5% Ru/γ-Al_2O_3 catalyst (T_{50} = 180 °C) [24]. From the presented results, it is obvious that much higher reaction temperature is required for CH_4 total

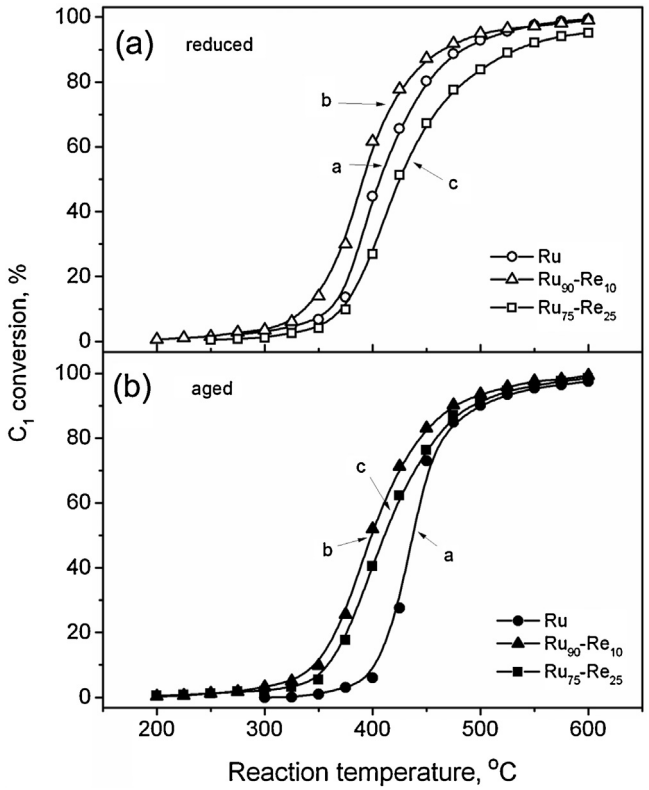

Fig. 7. Methane conversion as a function of temperature (a) over the reduced monometallic Ru and bimetallic Ru-Re catalysts (open symbols) and (b) over the aged monometallic Ru and bimetallic Ru-Re catalysts (full symbols). *Experimental conditions*: methane concentration: 0.8% vol. in air, total flow rate: 100 cm^3 min^{-1}; mass of the catalyst: 100 mg, pressure: atmospheric.

oxidation over the studied bimetallic Ru-Re and monometallic Ru catalysts because of the higher activation energy due to very strong C—H bond [38].

The effect of ageing treatment on methane conversion as a function of reaction temperature over the studied catalysts is presented in Fig. 7b. As it can be seen all air-aged catalysts exhibit slightly lower catalytic performance than the reduced samples (Fig. 7a). These results are in a good agreement with our recent report [32], in which we found that reduced Ru/$ZnAl_2O_4$ catalysts were more active than that treated in air at 300–800 °C. The T_{50} values for the both aged bimetallic Ru-Re catalysts were only 8–14 °C higher than those obtained for the reduced bimetallic samples, indicating a good stability of these catalysts under the reaction conditions. Opposite, for the aged Ru catalyst, the T_{50} value was about 30 °C

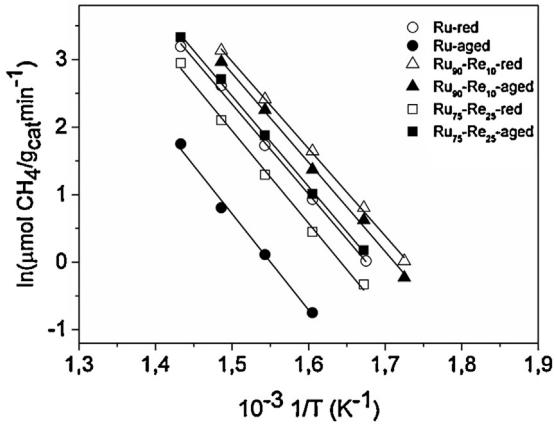

Fig. 8. Arrhenius-type plots for methane oxidation of the monometallic Ru and bimetallic Ru-Re catalysts. *Empty and full symbols* represent catalysts reduced in hydrogen at 500 °C and aged in air at 500 °C, respectively. *Experimental conditions*: methane concentration: 0.8% vol. in air, total flow rate: 100 cm^3 min^{-1}; mass of the catalyst: 100 mg, pressure: atmospheric.

higher as compared to that of the reduced sample (Table 4). Moreover, the aged bimetallic catalysts at both Ru/Re atomic ratios exhibit higher activity than the aged Ru catalyst and they show the initial steady state activity already at 200 °C, while the Ru catalyst at much higher temperature of 300 °C (Fig. 7b). Interestingly, it must be noted that the aged Ru_{75}-Re_{25} catalyst was even more active than the fresh one (T_{50} = 411 °C and 425 °C, respectively, Table 4). For the aged commercial Ru catalyst (Fluka), the light-off temperature (T_{50} = 436 °C) was similar to that in the fresh sample (Table 4). The superior catalytic performance of the bimetallic Ru-Re catalysts with the Re loading up to 3 wt.% is not a result of an additive effect of rhenium and ruthenium, since the 3% Re/γ-Al_2O_3 catalyst was completely inactive in this temperature range (Fig. 6d). Also, in a blank test, when only quartz wool was loaded in the reactor, no major conversion of CH_4 was observed below 500 °C what indicates that a contribution of a homogenous reaction could be neglected. We suppose that the differences in conversion curves in Fig. 7b should be partly explained by a variation in the amount of the exposed ruthenium surface since the Ru dispersion was enhanced when rhenium was added to the Ru/γ-Al_2O_3 catalyst (Table 3). A similar promotion effect of tungsten oxide and molybdenum oxide was found when Pt/Al_2O_3 catalyst was applied for methane combustion [39]. From density functional theory studies it was suggested that MoO_3 supported Pt catalysts can facilitate single C—H bond activation in methane [40]. Escandón et al. [41] also reported that the addition of 0.5% vanadium to the 1% Pd/γ-Al_2O_3 catalyst decreased the light-off temperature for methane oxidation, while a higher concentration led to lower conversion. The increase of the activity was explained by Pd–V interactions and a modification of the support properties. Opposite, Neyertz et al. [42] studied the influence of VO_x on catalytic properties of Pd catalysts and found that calcined Pd-VO_x/γ-Al_2O_3 catalysts, independent of the vanadium loading, exhibited lower activity for methane combustion than that of Pd/γ-Al_2O_3. Authors concluded that reconstruction of palladium, an essential requirement to form an oxidized phase, which is active for methane combustion, is inhibited by the presence of a VO_x monolayer.

Fig. 8 shows the Arrhenius plots of methane oxidation reaction for the reduced and aged monometallic Ru and bimetallic Ru-Re catalysts. The specific reaction rate used in the Arrhenius plots is expressed in micromoles of methane converted on 1 g of the catalyst per minute (μmol $g^{-}1$ min^{-1}). From the Arrhenius plots, apparent activation energies E_{app}, were calculated and summarized in Table 4. As it can be seen the activation energies are somewhat lower on the Re-modified Ru catalysts, indicating that addition of Re especially at 1 wt.%, slightly lowers the methane activation barrier. The E_{app} values of 104/105 kJ mol^{-1} were obtained for the reduced/aged bimetallic Ru_{90}-Re_{10} catalysts and nearly the same for the Ru_{75}-Re_{25} and monometallic Ru catalysts, (114/117 and 116/121 kJ mol^{-1}, respectively). For the commercial Ru catalyst (Fluka) the apparent activation energy (120 kJ mol^{-1}) was close to that of our home made Ru/γ-Al_2O_3 catalyst and similar to that found previously over the reduced and aged at 700 °C the Ru/$ZnAl_2O_4$ catalysts (121–129 kJ mol^{-1}) [18]. It can be noted that our values of the activation energies are higher as compared to those measured by Ribeiro et al. [43] on several supported Pd catalysts (76–92 kJ mol^{-1}) in a good agreement with higher activity of the Pd catalysts (Fig. 6). On the other hand, Beck et al. [44] found for the combustion of methane over the Pt/γ-Al_2O catalysts decreasing the apparent activation energy with diminishing mean particle size: 138 kJ mol^{-1} for d = 10.4 nm, 118 kJ mol^{-1} for d = 2.7 nm, 83 kJ mol^{-1} for d = 2.2 nm, and 67 kJ mol^{-1} for d = 1.3 nm. Methane total oxidation on these chlorine-free Pt/γ-Al_2O_3 catalysts was shown to be strongly size sensitive with the maximal TOF value observed for Pt crystallites of ca. 2 nm containing comparable amounts of partially oxidized and metallic platinum species. Additionally, it is clear from Fig. 8 that at the identical Ru loading (5 wt.%), the reduced bimetallic Ru_{90}-Re_{10} catalyst and both air-aged bimetallic catalysts are more active for methane combustion than the reduced/aged monometallic Ru catalyst. The large differences in the specific activity may indicate that the presence of rhenium influence the number of the active sites in these samples. However, no experimental data could be found in the literature to compare these results.

Some additional information about activity of the studied catalysts could be obtained by considering the specific reaction rate at given temperature, expressed as moles of CH_4 converted per gram of the catalyst and per minute. The turnover frequencies values (TOF, molecules of methane reacted per surface Ru per second) of the catalysts cannot be taken into account since the particle size of the Ru phase can change not only in the air atmosphere (Table 3), but also during course of the reaction under oxygen-rich conditions. Table 4 shows that at the reaction temperature of 350 °C (in the kinetic region), the reduced bimetallic Ru_{90}-Re_{10} catalyst exhibits twofold enhancement in the specific reaction rate (5.17 μmol g^{-1} min^{-1}) relative to the reduced monometallic Ru catalyst (2.53 μmol g^{-1} min^{-1}). However, the methane oxidation rate over the aged Ru_{90}-Re_{10} catalyst was found about ten times higher (3.65 μmol g^{-1} min^{-1}) compared to that of the aged Ru catalyst (0.37 μmol g^{-1} min^{-1}). Slightly smaller enhancement in the methane oxidation rate (∼5×) was observed for the aged bimetallic Ru_{75}-Re_{25} catalyst (Table 4). Thus, the pretreatment in air at 500 °C has a beneficial effect on the specific activity of the bimetallic Ru-Re catalysts in combustion of methane in comparison to the Ru sample. Such a catalytic behaviour could be associated with better dispersion of the aged bimetallic catalysts and also good reducibility (Fig. 5). In reality, the TEM observations (Fig. 3) and XRD data (Fig. 2) point out that the aged bimetallic catalysts were more effective for maintaining a higher dispersion of the active Ru phase. We suppose that at reaction conditions rhenium is predominantly situated on the surface of the alumina support and only small part of the oxidized ReO_x species may be located on the surface of RuO_2 oxide forming RuO_2-ReO_x species as shown by the STEM-HAADF observations. Therefore, the changes in activity can be mainly attributed to a geometric effect although some influence of an electronic interaction between the two metals could not be excluded as shown by TPR measurements (Fig. 5). Additionally, the presence of a high number of very small ReO_x species all over the surface of the alumina support (Fig. 4) partly prevents agglomeration of the Ru particles, thus improving the catalytic performance of the bimetallic catalysts.

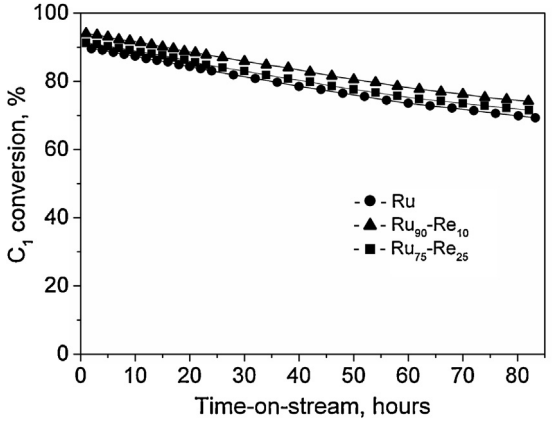

Fig. 9. Methane conversion over the aged $Ru/\gamma\text{-}Al_2O_3$ catalyst (●) and the aged bimetallic $Ru_{90}\text{-}Re_{10}/\gamma\text{-}Al_2O_3$ (▲) and the $Ru_{75}\text{-}Re_{25}/\gamma\text{-}Al_2O_3$ (■) catalysts as a function of time on stream at constant temperature 500 °C.

3.3.1. Catalyst durability

In order to investigate the influence of rhenium on the long-term activity of the bimetallic catalysts in comparison with that of the monometallic Ru sample, experiments were performed for up to 80 h. Although hundreds of studies are available on methane combustion over supported metal catalysts, not many of them deal with longer term testing. Fig. 9 shows methane conversion over the studied catalysts as a function of time on stream at constant temperature of 500 °C. These results were obtained over the catalyst samples after ageing treatment at 500 °C. A constant decrease in the methane conversion was observed both in the case of monometallic and bimetallic catalysts. For the monometallic Ru catalyst, the initially high conversion of 90% drops to only 69% after 80 h. A slightly smaller drop of the methane conversion was observed for the both bimetallic Ru-Re catalysts i.e., from 95 to 93% to about 73–71%. In Supplementary material methane conversion over the reduced catalysts as a function of time on stream at constant temperature of 500 °C is presented (Fig. S1). As shown, a greater drops in methane conversion is observed for reduced catalysts compared to the aged samples (Fig. 9). A deactivation of noble metal catalysts, including the most active Pd catalysts, during methane oxidation is a common phenomenon. Most frequently, deactivation of the Pd-based catalysts is related to the Pd sintering, transformation of active PdO to Pd^0 at high temperature or occlusion by support species [45,46].

In our case in order to clarify the reasons of deactivation of the Ru-based catalysts we took into consideration: (1) changes of the BET surface area during high temperature methane combustion, (2) loss of the Ru or Re oxides by volatilization during heating under a CH_4/O_2 mixture at high temperature, and (3) possible changes in the structure of the catalysts. Therefore, the deactivated catalyst samples after the long-term activity tests and also all samples after the first catalytic test were characterized by nitrogen adsorption-desorption measurements, EDS and XRD techniques. In fact, some literature data show that a drop of the BET surface area during methane combustion reaction may deactivate metal catalysts to some extent [47]. In our study, no major differences were observed in the BET surface areas of the catalyst samples before and after catalytic tests. As shown in Table 2, the BET surface areas varied between 172 and 159 m^2/g for the used fresh reduced $Ru/\gamma\text{-}Al_2O_3$ and $Ru\text{-}Re/\gamma\text{-}Al_2O_3$ catalysts, but for the all used aged catalysts the BET surface areas are nearly the same (144–148 m^2/g) as before the catalytic tests (145–149 m^2/g). Therefore, the observed some catalyst deactivation is not caused by the changes in the support structure. Also, EDS data presented in Table 1 indicated that composition and the Ru/Re atomic ratios in the used bimetallic catalysts, both reduced or air-aged, are close to those in the fresh samples, confirming that no noticeable loss of Ru and Re (as volatile RuO_4 or Re_2O_7 oxides, respectively) occurred during the course of methane combustion up to 600 °C. It is well known that pure Re_2O_7 sublimes above 200 °C [48]. However, it appears that strong interaction of Re with γ-alumina support prevents its loss from the catalyst even at high temperature. We previously studied the interaction of oxygen with the reduced monometallic $Re/\gamma\text{-}Al_2O_3$ catalyst over a wide temperature range (20–800 °C), and it was found that only at 800 °C a part of Re oxide sublimes as Re_2O_7 [27]. The literature data reported that also some Ru loss in the unsupported RuO_2 oxide and in supported Ru catalysts, by volatilization of RuO_4 above 800 °C occurred in air-atmosphere [35]. In the present study we performed catalytic tests at lower temperature (maximum 600 °C) and we did not observe Re or Ru loss in the fresh and aged bimetallic catalysts.

Structure characterization of the used catalysts by XRD show that after the first catalytic test, all the Ru and Ru-Re catalysts, which were in O_2-rich reaction conditions for about 10 h, exhibited the XRD patterns with the diffraction peaks of RuO_2 oxide. XRD patterns, shown in the Supplementary material (Figs. S2 and S3), are similar to those obtained after the ageing treatment (Fig. 2). The mean crystallite size of RuO_2 oxide, formed during methane combustion reaction over the reduced Ru and bimetallic Ru-Re catalysts was similar and amounted to 25–27 nm (Fig. S2, Table 3, last column). For the used aged Ru and $Ru_{90}\text{-}Re_{10}$ catalysts the crystallite size of RuO_2 was slightly higher (32–31 nm), and only for the used aged $Ru_{75}\text{-}Re_{25}$ catalyst it was much lower and amounted to 23 nm (Fig. S3, Table 3). These results are in good agreement with the activity data (Fig. 7), which show that air-aged catalysts, except of the $Ru_{75}\text{-}Re_{25}$ catalyst, exhibited slightly lower catalytic performance than that of the reduced samples. Interestingly, in the all used Ru-based catalysts, independent of the pretreatment procedure, the mean size of the RuO_2 crystallites was close to that after air treatment at 500 °C for only 3 h (Table 3). The above presented XRD data clearly indicate that deactivation of the bimetallic Ru-Re catalysts due to nanoparticle sintering is only insignificantly smaller with respect to the monometallic Ru catalysts. Recently, we found that addition of Re significantly suppressed Ru particle sintering in the $Ru\text{-}Re/\gamma\text{-}Al_2O_3$ catalysts during propane combustion reaction [24]. However, oxidation of propane over Ru-based catalysts was complete at much lower temperature (below 250 °C), but complete catalytic oxidation of methane was possible at temperature even higher than 550 °C (Fig. 7 and Table 4).

The deactivated aged Ru and Ru-Re catalyst samples after the long-term activity tests (80 h) at 500 °C exhibited the XRD patterns (Supplementary material, Fig. S4) with more intensive and narrow diffraction peaks of the RuO_2 phase. For the used monometallic Ru catalyst the mean crystallite size of RuO_2 amounts to 45 nm, while for the used $Ru_{90}\text{-}Re_{10}$ and $Ru_{75}\text{-}Re_{25}$ catalysts it amounts to 44 or 40 nm, respectively. Therefore, it is evident that deactivation process of the both monometallic Ru and bimetallic Ru-Re catalysts (Fig. 9) is mainly caused by the loss of the active surface area of ruthenium due to sintering of the Ru phase and formation of large RuO_2 crystallites.

4. Conclusions

Combustion of methane was performed for the first time using bimetallic $Ru\text{-}Re/\gamma\text{-}Al_2O_3$ catalysts after reduction in hydrogen or ageing treatment in air and compared to the $Ru/\gamma\text{-}Al_2O_3$ catalyst. The results shows that pre-treatment procedures have a significant influence on the catalytic activity of the studied catalysts. At the identical Ru loading (5 wt.%), the reduced bimetallic $Ru_{90}\text{-}Re_{10}$ catalyst and both air-aged bimetallic catalysts were more active for methane combustion than the reduced/aged monometallic Ru catalyst. The characterization data revealed that higher activity of the

Re-containing catalysts may be attributed to the higher dispersion of the Ru phase and good reducibility. However, at high reaction temperature of 500 °C, a gradual deactivation of the both bimetallic Ru-Re and Ru catalysts was observed (20% drop in the methane conversion was seen in 80 h). Therefore, although the addition of Re increases the catalytic activity of the binary Ru-Re catalysts in methane combustion but does not affect the stability of the catalysts which is similar to that of the monometallic Ru catalyst.

Acknowledgements

The authors thank Mrs. E. Bukowska for XRD, Dr. K. Rola for SEM-EDS and Mrs. L. Krajczyk for TEM measurements. The STEM-HAADF study received funding from the European Union Seventh Framework Programme under Grant Agreement 312483—ESTEEM2 (Integrated Infrastructure Initiative—13). This work was financially supported by the National Science Centre in Poland (Grant no. UMO-2012/07/B/ST5/02028).

Appendix A. Supplementary data

Supplementary data associated with this article can be found, in the online version, at http://dx.doi.org/10.1016/j.apcatb.2016.04.038.

References

[1] R. Burch, D. Crittle, M. Hayes, Catal. Today 47 (1999) 229–237.
[2] M. Lyubovsky, L.L. Smith, M. Castaldi, H. Karim, B. Nentwick, S. Etemad, R. LaPierre, W.C. Pfefferle, Catal. Today 83 (2003) 71–84.
[3] J. Chen, H. Arandiyan, X. Gao, J. Li, Catal. Surv. Asia 19 (2015) 140–171.
[4] J. Nilsson, P.A. Carlsson, S. Fouladvand, N.M. Martin, J. Gustafson, M.A. Newton, E. Lundgren, H. Grönbeck, M. Skoglundh, ACS Catal. 5 (2015) 2481–2489.
[5] S. Specchia, E. Finocchio, G. Busca, P. Palmisano, V. Specchia, J. Catal. 263 (2009) 134–145.
[6] S.H. Oh, P.J. Mitchell, Appl. Catal. B: Environ. 5 (1994) 165–179.
[7] N.M. Kinnunen, M. Suvanto, M.A. Moreno, A. Savimäki, K. Kallinen, T.J.J. Kinnunen, T.A. Pakkanen, Appl. Catal. A: Gen. 370 (2009) 78–87.
[8] J. Bassil, A. AlBarazi, P. Da Costa, M. Boutros, Catal. Today 176 (2011) 36–40.
[9] K. Narui, H. Yata, K. Furuta, A. Nishida, Y. Kohtoku, T. Matsuzaki, Appl. Catal. A: Gen. 179 (1999) 165–173.
[10] K. Persson, A. Ersson, K. Jansson, J.L.G. Fierro, S.G. Jära°s, J. Catal. 243 (2006) 14–24.
[11] R. Strobel, J.-D. Grunwaldt, A. Camenzind, S.E. Pratsinis, A. Baiker, Catal. Lett. 104 (2005) 9–16.
[12] Y. Reneme, F. Dhainaut, S. Pietrzyk, M. Chaar, A.C. van Veen, P. Granger, Appl. Catal. B: Environ. 126 (2012) 239–248.
[13] X.N. Guo, P. Brault, G.J. Zhi, A. Caillard, G.Q. Jin, C. Coutanceau, S. Baranton, X.Y. Guo, J. Phys. Chem. C 115 (2011) 11240–11246.
[14] T.V. Choudhary, S. Banerjee, V.R. Choudhary, Appl. Catal. A: Gen. 234 (2002) 1–23.
[15] S. Aouad, E. Abi-Aad, A. Aboukaïs, Appl. Catal. B: Environ. 88 (2009) 249–256.
[16] Ch.K. Ryu, M.W. Ryoo, I.S. Ryu, S.K. Kang, Catal. Today 47 (1999) 141–147.
[17] H. Ohtsuka, Catal. Lett. 143 (2013) 1043–1050.
[18] J. Okal, M. Zawadzki, Appl. Catal. A: Gen. 453 (2013) 349–357.
[19] N.M. Kinnunen, J.T. Hirvi, M. Suvanto, T.A. Pakkanen, J. Mol. Catal. A: Chem. 356 (2012) 20–28.
[20] P. Hurtado, S. Ordónez, A. Vega, F.V. Díez, Chemosphere 55 (2004) 681–689.
[21] L. Ma, D. He, Topics Catal. 52 (2009) 834–844.
[22] L. Ma, D. He, Catal. Today 149 (2010) 148–156.
[23] K. Baranowska, J. Okal, N. Miniajluk, Catal. Lett. 144 (2014) 447–459.
[24] K. Baranowska, J. Okal, Appl. Catal. A: Gen. 499 (2015) 158–167.
[25] K. Baranowska, J. Okal, Catal. Lett. 146 (2016) 72–81.
[26] S. Albonetti, F. Cavani, F. Trifiro, Catal. Rev. Sci. Eng. 38 (1996) 413–438.
[27] J. Okal, L. Kępiński, L. Krajczyk, M. Drozd, J. Catal. 188 (1999) 140–153.
[28] G. Beamson, A.J. Papworth, Ch. Philips, A.M. Smith, R. Whyman, J. Catal. 278 (2011) 228–238.
[29] K.H. Kang, U.G. Hong, Y. Bang, J.H. Choi, J.K. Kim, J.K. Lee, S.J. Han, I.K. Song, Appl. Catal. A: Gen. 490 (2015) 153–162.
[30] D. Roth, P. Gelin, E. Tena, M. Primet, Topics Catal. 16/17 (2001) 77–82.
[31] K. Narui, K. Futura, H. Yata, A. Nishida, Y. Kohtoku, T. Matsuzaki, Catal. Today 45 (1998) 173–178.
[32] J. Okal, M. Zawadzki, K. Baranowska, Appl. Catal. A: Gen. 471 (2014) 98–105.
[33] M.A. Yuurman, D.J. Stufkens, A. Oskam, I.E. Wachs, J. Mol. Catal. 76 (1992) 263–285.
[34] J. Okal, W. Tylus, L. Kępiński, J. Catal. 225 (2004) 498–509.
[35] R. Lanza, S.G. Järas, P. Canu, Appl. Catal. A: Gen. 325 (2007) 57–67.
[36] S. Koso, H. Wanatabe, K. Okumura, Y. Nakagawa, K. Tomishige, J. Phys. Chem. C 116 (2012) 3079–3090.
[37] Y. Amada, H. Watanabe, M. Tamura, Y. Nakagawa, K. Okumura, K. Tomishige, J. Phys. Chem. C 116 (2012) 23503–23514.
[38] Y.-H. Chin, C. Buda, M. Neurock, E. Iglesia, J. Am. Chem. Soc. 135 (2013) 15425–15442.
[39] M. OíConnell, G. Kolb, R. Zapf, Y. Men, V. Hessel, Catal. Today 144 (2009) 306–311.
[40] Z. Jiang, W. Huang, H. Zhao, Z. Zhang, D. Tan, X. Bao, J. Mol. Catal. A: Chem. 268 (2007) 213–220.
[41] L.S. Escandón, S. Ordoñez, F.V. Diez, H. Sastre, Catal. Today 78 (2003) 191–196.
[42] C. Neyertz, M. Volpe, C. Gigola, Appl. Catal. A: Gen. 277 (2004) 137–145.
[43] F. Ribeiro, M. Chow, R. Dalla Betta, J. Catal. 146 (1994) 537–544.
[44] I.E. Beck, V.I. Bukhtiyarov, I.Y. Pakharukov, V.I. Zaikovsky, V.V. Kriventsov, V.N. Parmon, J. Catal. 268 (2009) 60–67.
[45] R. Gholami, M. Alyani, K.J. Smith, Catalysis 5 (2015) 561–594.
[46] A.T. Gremminger, H.W.P. de Carvalho, R. Popescu, J.D. Grunwaldt, O. Deutschmann, Catal. Today 258 (2015) 470–480.
[47] P. Gélin, M. Primet, Appl. Catal. B: Environ. 39 (2002) 1–37.
[48] X.D. Xu, C. Boelhouver, J.I. Benecke, D. Vonk, J.C. Mol, J. Chem. Soc. Faraday Trans. 1 (82) (1986) 1945–1953.